Chronology and orientation of N_2–CH_4, CO_2–H_2O, and H_2O-rich fluid-inclusion trails in intrametamorphic quartz veins from the Cuiabá gold district, Brazil

C. J. S. DE ALVARENGA*

Departamento de Geologia, Universidade Fed. de Mato Grosso, Cuiabá, 78100, Brazil

M. CATHELINEAU AND J. DUBESSY

CREGU and GS CNRS-CREGU, BP 23,54500, Vandoeuvre-les-Nancy, France

Abstract

The upper Proterozoic Cuiabá group of Mato Grosso, Brazil, is composed of low-grade clastic meta-sediments which have been folded by several successive tectonic events. Three generations of quartz veins are associated with the structural evolution of this area. The first veins are deformed by the main tectonic phases and show a complex deformational patterns. The second set is parallel to the cleavage and was formed syntectonically during the main folding phase, whilst the last quartz veins are related to a later stage of deformation. A systematic study of fluid inclusions in relation with a statistical study of microstructural markers (fluid inclusion trails, opened microcracks) was carried out on quartz veins from three localities. On the basis of microthermometric studies and Raman spectrometry analysis, four differents types of fluids have been distinguished, each trapped in specific fluid inclusion trails: (i) CO_2-rich liquids and vapours (Lc, Vc) at Casa de Pedra, (ii) Lc and Vc inclusions with variable amounts of CO_2, CH_4, N_2 in the vapour phase at BR-70, (iii) CH_2–N_2-rich vapours (Vn-m), and (iv) aqueous inclusions (L) with variable salinities representing the last fluid generations at all localities.

At Casa de Pedra and BR-70, most fluids are observed within the three generations of quartz veins, indicating an important fluid circulation associated with the last phase of brittle deformation. Fluid inclusions of type (iii) and (iv) are oriented along several well defined directions. The study shows the importance of integrated microstructural and fluid-inclusion studies for understanding the geometry and chronology of fluid circulation.

KEYWORDS: fluid-inclusion trails, quartz veins, gold, Brazil.

Introduction

FLUIDS generated during low-to medium-grade metamorphism have been relatively well documented in the past few years (Roedder, 1984; Crawford and Hollister, 1986; and Mullis, 1979, 1987). However, very few data on the geometry of fluid migration linked to time–space relationships between deformational events and regional metamorphism are available. In particular, the relationships between fluid migration during ductile to late brittle deformation are relatively poorly known.

The identification of fluid inclusions within healed micro-fractures was first recognized by Tuttle (1949). Later, Wise (1964), Pêcher et al. (1985), Lespinasse and Pêcher (1986), and Kowallis et al. (1987) related the different stages of fluid activity with microfracturing and regional deformational events.

The Cuiabá province in Brazil provides an interesting example of successive crystallization

* Present address: Lab. de Géologie Dynamique et Petrologie de la Surface, Centre de St. Jérôme, 13397 Marseille, France.
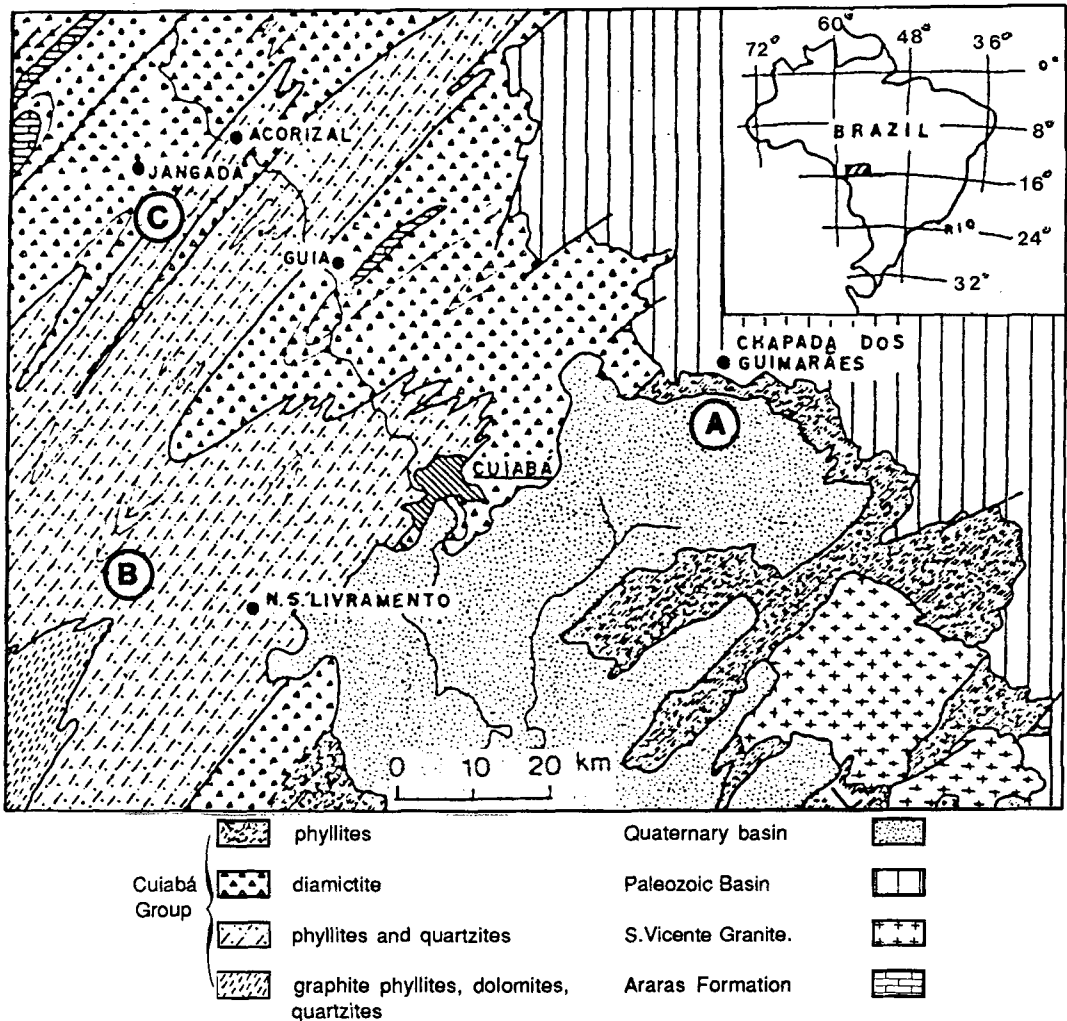
FIG. 1. Geological map of the Paraguay Belt in the Cuiabá area showing sample locations. A (Casa de Pedra), B (BR-70), and C (Jangada).

and microfracturing of quartz veins in metamorphic series during a multistage deformation. The study of fluid inclusions in relation with deformation structures may provide *a priori* useful data for the reconstruction of the *P–T* conditions during metamorphism and deformation. Such data are especially needed in the case of metamorphic series characterized by fine-grained phyllites, the mineralogy of which does not give any geothermobarometric constant for metamorphic stages. This paper discusses the evolution of physical–chemical conditions during fluid migration in relation with microfracturing, and the difficulties in identi-

fying relics of the earliest fluids which are generally overprinted.

Geological setting of the Cuiabá quartz veins

The study was carried out on quartz veins from the Cuiabá Group, Mato Grosso state (middle-west Brazil, Fig. 1). The Cuiabá Group is a thick sequence of diamictites, phyllites, quartzites, graphite phyllites with local pebble conglomerates, which have been affected by low-grade metamorphism determined by recrystallization of the clay-size minerals (illite, chlorite and other phyllosilicates) parallel to cleavage planes. This group has

Table 1 : Geological framework for host rocks and quartz veins in the Cuiabá Group.

Age of the host rock	Upper-Proterozoic Cuiabá Group		
Host rock	Low-grade metasedimentary rocks		
Metamorphism of host rock	Deformation and regional metamorphism --------increasing metamorphism------->		
Locations	Jangada	BR - 070	Casa de Pedra
Vein 1 (i)		Pre or syn-deformational quartz veins (folded with regional structures, D1)	
Vein 2 (ii)		Syn-deformational quartz veins (parallel to the regional structures, D1)	
Vein 3 (iii)	Late vertical quartz veins (Cross cutting, perpendicular to veins 1 and 2 when present)		
Late microfracturing , brittle deformation stage			

been folded and metamorphosed by the Brasiliano orogeny, dated at *c.* 600 Ma elsewhere. However, recent data suggest a maximum age of 550 Ma in the Cuiabá region (Alvarenga and Trompette, in press).

The metasedimentary rocks represent an uppermost Proterozoic marine basin with glacial influenced turbidite sedimentation (Alvarenga, 1988; Alvarenga and Trompette, in press). Most of the gold-bearing veins quartz are emplaced in fine-grained sediments hosted by turbidites.

A few post-orogenic granitic intrusions are present in the eastern part of the Paraguay Belt which is represented in the study area by the São Vicente Granite. This body has a metamorphic hornfels aureole of variable width, ranging from ten to a few hundred metres (Almeida and Mantovani, 1975). The São Vicente Granite has been dated at 500 ± 15 Ma by whole rock K/Ar and Rb/Sr methods (Hasui and Almeida, 1970; Almeida and Mantovani, 1975).

Tectonic context

Four closely related phases of regional deformation (D1 to D4) are distinguished in the Paraguay Belt (Alvarenga, 1986). The trend directions of D1, D2 and D3 are almost identical (NE–SW) whereas D4 is transverse (NW–SE). The first phase D1 is the most prominent, and is contemporaneous with the regional metamorphism. It produced tight and isoclinal F1 folds (eastern) to open folds F1 (western), and associated S1 clea-

vage. The D2 phase consists mainly of local penetrative crenulation cleavages (S2). D3 phase displays open fold with upright contemporaneous crenulation and fracture cleavage. D4 phase is characterized by slight transverse folds.

The three localities studied exhibit rather similar deformational patterns, and almost identical preferred orientations of deformation markers (fold axis, cleavage, and brittle structures).

Quartz veins

Three main generations of quartz veins can be distinguished within the low-grade, fine-grained metasediments of the Cuiabá Group (Table 1). Early veins (i) are folded concordantly with the D1 regional structures. They are present at Casa de Pedra with fold axis directions oriented N 60°E, and N 45°E at locality BR-70. The second generation (ii) is parallel to the regional cleavage S1, and have orientations N 45° E 50 NW, at BR-70 and around N 60 °E 35 NW at Casa de Pedra. Later vertical veins (iii), oriented N 125° E are associated with the D4 phase. They are observed everywhere crosscutting beddings, cleavages, and early veins.

In the eastern zone of the province (Fig. 1), D4 quartz veins are auriferous (Casa de Pedra mine), whilst some Au occurrences have been found in outcrops near the locality BR-70. Folded veins are sometimes mineralized (Campos *et al.*, 1987). In the western zone, at Jangada, quartz veins are barren.
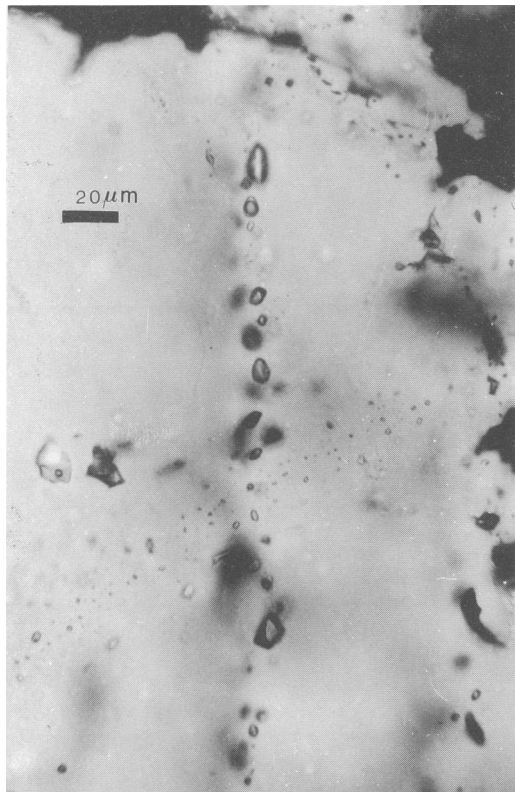
FIG. 2. N_2–CH_4 (Vm-n) F.I.T. cross-cut by a later aqueous (L) F.I.T.

Analytical methods

Fluid inclusions analysis

Fluid inclusions were studied by microthermometry and Raman spectrometry (Dubessy *et al.*, 1989), on 14 milky quartz samples representative of (i, ii, iii) veins. The same samples were used for microfracture analysis. All fluid inclusions are found within F.I.T.

Microthermometric studies were made using the Chaix-Meca heating–freezing stage (Poty *et al.*, 1976) on 150 fluid inclusions. Salinities, expressed in wt.% NaCl, were determined by microthermometry (Potter, 1977; Potter *et al.*, 1978), and all measurements were corrected to a standard calibration curve. Molar fractions of CO_2, CH_4, H_2S and N_2 were determined in individual inclusions by micro-Raman analysis performed on DILOR X-Y, multichannel Raman spectrometer.

Fluid inclusions are described using the following symbols: CO_2 (c), N_2 (n), CH_4 (m), homogenization temperatures to liquid (L), or to vapour (V).

Geometry of the microstructural markers

Systematic measurements of microstructural markers (cracks and fluid inclusions trails—F.I.T.) were carried out in horizontal sections from orientated samples. About 40% of the thin sections were studied at CRPG-Nancy using an interactive videographic analyser, PC microcomputer (Lapique *et al.*, 1988); 30% using an image treatment device (Oltra, 1988) at the Faculty of St. Jérôme–Marseille, and 30% by hand. F.I.T. have been mostly studied from quartz veins and where possible, in quartzite host rocks. Orientation analysis takes into account the nature of the crack, and the nature of the fluid inclusions, in the favourable cases. Results are given in rose diagrams for each kind of microcrack and F.I.T.

Fluid inclusions

Typology and analytical results

Five types of inclusions are distinguished on the basis of textural relationships, and the data from microthermometry and Raman spectroscopy. The results are summarized in Tables 2 and 3.

CO_2-rich fluids. At Casa de Pedra, CO_2 was identified either by Tm CO_2, Th CO_2, Tm clathrate or Raman analysis in CO_2-rich liquids (Lc) and vapours (Vc). The size of these inclusions ranges from less than 4 μm to 20–30 μm. Tm CO_2 lower than −56.6 °C indicates the presence of other gases, mostly N_2, as later identified by Raman analysis. Bulk homogenization (H) occurs to the liquid (Lc) or vapour state (Vc). Careful examination reveals the following points. Lc inclusions are of two types: some have a high density CO_2 phase (homogenization to liquid–Lcl) whereas others have a low CO_2 density phase (Lcv). Lcl inclusions occur in restricted zones of the sample, with no associated Vc inclusions. They homogenize in the range 250–350 °C. Lcv inclusions, with low density CO_2 are very often associated with some Vc inclusions in the same healed fractures. In this case, bulk homogenization temperatures of Lcv and Vc inclusions occur within a 30–40 °C temperature range around 380 °C.

In BR-70 samples, Lc and Vc inclusions are two-phase (liquid H_2O and vapour), exhibiting variable filling degrees, ranging from 10% to 90%, and an average size from less than 5 μm to 20 μm. $TmCO_2$ and $ThCO_2$ were never observed by microthermometric analysis, whilst rare Tm (clathrate) were noted (Table 2). Raman analysis shows a low-density vapour phase with variable amounts of CO_2, CH_4, N_2 (Fig. 3).

(CH₄-N₂)-rich vapours. Methane–nitrogen rich

Table 2. Microthermometric data. TmCO$_2$; melting temperature of CO$_2$ in presence of liquid and vapours. TmI ; melting temperature of H$_2$O. TmC ; melting temperature of clathrate. Th ; homogenization temperature of CO$_2$*. TH ; bulk homogenization temperature. l ; homogenization to liquid. v ; homogenization to vapour. All values in °C. Bold character ; average value. d; density (g/cm^3). *Measured only in three-phase inclusions.

Type of inclusion		Jangada (C)		BR - 7 0 (B)				Casa de Pedra (A)			
		perpendicular		folded		perpendicular		folded		perpendicular	
CO2-H2O (Lcl-Lcv-Vc)	TmCO2							-57,5/-60,0	**-5 9**	-57,5/-59,5	**-5 9**
	Tm I			-5,0/-8,0	**-6**	-5,0/-18,0	**-6**	-0,7/-8,0	**-4,3**	-3,0/-7,5	**-4,3**
	TmC			7,0/7,5	**7,5**	7,0/7,5	**7,5**	7,0/10,5	**8,5**	4,5/10,0	**9**
	Th CO2*							12,7/21,5 (l,v)	**15,5**	13,1/21,5 (v)	**1 9**
	TH			280/360 (l)	**3 4 0**	260/410 (l,v)	**3 4 0**	240/420 (l,v)	**3 8 0**	260/400 (l,v)	**3 2 0**
N2-CH4 (Vn-m)	T H			-113/-126 (v)	**-1 1 6**	-113/-122 (v)	**-1 1 7**				
H2O (L)	wt % NaCl eq.	0,67/3,37	**2,2 3**	4,94/13,44	**7,9 5**	3,37/17,0	**8,5 4**	1,73/4,94	**3,3 7**	0,5/5,70	
	Tm I	-0,5/-2,0	**-1,3**	-3,0/-9,5	**-5**	-2,0/-13,0	**-5,5**	-1,0/-3,0	**-2**	-0,3/-3,5	
	T H	100/160 (l)	**1 3 0**	140/200(l)	**2 0 0**	140/250 (l)	**1 6 0**	120/240	**1 9 0**	140/240	**1 9 0**
	d	0,92/0,94	**0,9 3**	0,85/0,93	**0,9 1**	0,81/0,93	**0,9**	0,86/0,93	**0,8 8**	0,84/0,91	**0,8 8**

vapours (Vn–m) were only found in samples from BR-70 (Fig. 2). They exhibit regular shapes (subrounded to elliptical), many having a negative crystal shape. Their size is in the range 5–20 μm. Homogenization of N$_2$–CH$_4$ (Th n–m) is to the vapour phase between −114 and −126 °C with a mean value of −116.5 °C. The scattering of homogenization temperature is quite low (±1 °C) in a given trail.

Aqueous inclusions. These inclusions (L) were observed at all localities. They are two-phase inclusions with a degree of filling around 80–95%. TH of L inclusions are in the range 120–260 °C, but TH mode decreases significantly from Casa de Pedra (180 °C) to BR-70 (160 °C) and Jangada (120 °C) (Fig. 4).

The Tm–TH plot (Fig. 5) shows that the higher TH values characterize the carbonaceous inclusions, Vc, Lcv from BR-70 and Casa de Pedra, whilst lower TH values are obtained on all L inclusions from the three localities. At BR-70, Tm ice values are significantly higher than those at Casa de Pedra and Jangada. The Tm of the aqueous phase is relatively constant within a given locality, whatever the type of inclusions, Vc, Lc, or L. The only exception concerns some rare L inclusions fron BR-70 which display lower Tm in the range −9 to −11 °C.

Bulk chemical composition

Bulk chemical compositions and density of three-phase fluid inclusions have been calculated using the methodology developed by Ramboz *et al.* (1985) and Dubessy *et al.* (1989) from Raman and microthermometric data (Table 4).

It was not possible to calculate bulk V–X properties in two-phase inclusions with low-density CO$_2$–CH$_4$–N$_2$ vapour phases using the above methods. However, a crude estimation of the gas content can be made from available phase diagrams and homogenization temperatures. In Lc inclusions with TH ≈ 350 °C, the gas content is probably 5–10 mole % and in Vc inclusions with TH ≈ 400 °C, the gas concentration is probably 40–60 mole %. Ice melting temperatures could not be measured for the Vc inclusions, but their TH are higher than critical temperatures of the H$_2$O–gas system, thus indicating a fall in salinity for this Vc inclusion.

N$_2$–CH$_4$-rich inclusions also contain small amounts of CO$_2$ and H$_2$S. Liquid water is not visible, indicating a very low water content. In the absence of thermodynamic data of the V–X properties of L–V equilibrium in the system N$_2$–CH$_4$ and the unknown water content, bulk V–K properties could not be calculated for this type of inclusion.

Variations in density of L inclusions were calculated from the algorithm of Zhang and Frantz (1987) and are given in Table 2.

Relative chronology of fluid inclusions

Casa de Pedra. Lc and Vc inclusions define oriented healed microfractures of small extension
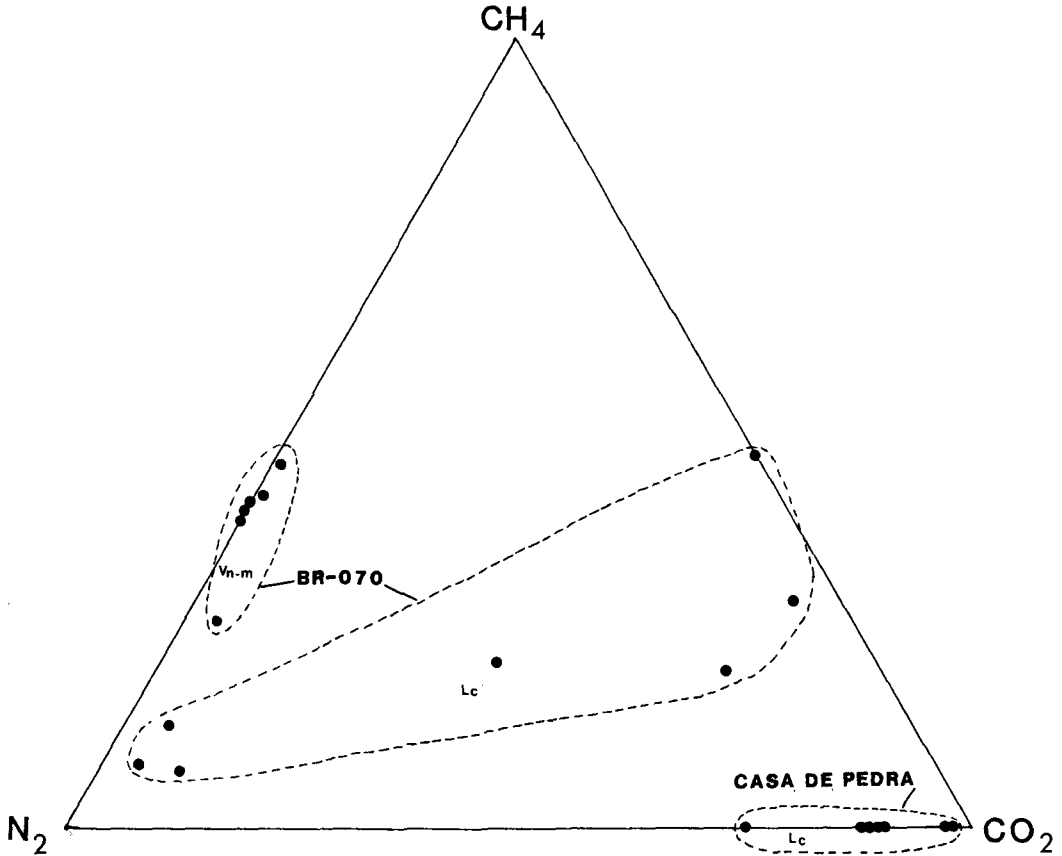
FIG. 3. Triangular diagram showing the chemical compositions of gas phase in fluid inclusions obtained by Raman microprobe spectrometry.

inside individual quartz crystals. By contrast, aqueous F.I.T. (L) crosscuts several quartz crystals. These features clearly demonstrate that Lc–Vc inclusions were formed before L inclusions (Fig. 6). When samples are studied separately, the orientation of microcracks are within 10° of the orientation of L type F.I.T. (Table 5). This suggests that microcracks and aqueous F.I.T. result from the same tectonic event. The lack of healing of some microcracks may be due to the low temperature at which this brittle deformation occurred.

BR-70. At this locality three types of F.I.T. have been recognized. Lc and Vc inclusions exhibit the same pattern as for Casa de Pedra. Single phase N_2–CH_4 inclusions occur along long F.I.T. which never cross-cut quartz grain boundaries (Fig. 6). Aqueous F.I.T. crosscut several quartz crystals as at Casa de Pedra. In addition, L inclusions clearly cross-cut N_2–CH_4 inclusions (Fig. 2).

Therefore, the probable chronology is the following: (1) Lc–Vc inclusions; (2) N_2–CH_4 inclusions; (3) aqueous inclusions.

Jangada. L type aqueous inclusions, with a single TH mode, are the only inclusions observed and occupy the F.I.T. They display the same features as those from the other localities.

At high magnification, aqueous inclusions often seem to be mixed with trails of previous inclusions at Casa de Pedra and BR-70. This results probably from late and intense reopening/rehealing process affecting a part of the earlier microstructures.

Microthermometric and Raman spectrometry data show that at each locality, F.I.T. containing the same type of fluid inclusions have been observed either in the folded quartz veins (i, ii) or late cross-cutting quartz veins (iii). Thus, all trapping stages are just later than the late quartz vein crystallization and correspond to stages of brittle deformation.

Table 3 : Chemical compositions of the volatile phase analysed by Raman spectrometry and microthermometric data of inclusions . (i) : folded veins, (ii) : veins parallel to cleavage, (iii) : vertical veins orthogonal to main regional direction, L : homogenization to liquid, V : homogenization to vapour.

Locations	Type of veins	CO2	CH4	N2	H2S	Tm CO2 °C	Th CO2 °C	Tm C °C	Th N2 °C	Tm H2O °C	TH °C
B R	(i)	3,5	26	70	0,3				-115 V		
	(i)		40	60	0,3				-126 V		
	(iii)	0,7	42	57	0,2				-116 V		
	(iii)	0,6	46	53	0,4				-115 V		
	(ii)	0,3	39	60	0,3				-119 V		
	(ii)	0,5	40	59	0,2				-119 V		
7 0	(ii)	66	29	5							
	(iii)	53	47								
	(i)	37	21	42				5		-8,5	
	(i)	4	8	88							
	(i)	5	13	82							
	(i)	9	7	84							
	(iii)	63	20	17				7,5		-7	
C P E D R A	(iii)	96		4		-59	18,6 V	9,5			266 L
	(iii)	93		7		-58,3	22 V	8,5			
	(ii)	76		24				9,1			350 L
	(i)	90		10		-57,5	20,5 V	9,5			
	(i)	89		11		-56,9		7,5			
	(iii)	88		12		-58,6	13,1 V	4,5			385 V
	(ii)	90		10		-59,1	17,7 L	8,5			

Microfracturing and F.I.T. geometry

Table 5 summarizes the main results obtained on the geometry of microstructural markers for quartz veins and host rocks.

In most samples, there is a strong relationship between microstructure orientations (F.I.T. and microcracks) and macro-regional structures: (1) One of the main F.I.T. directions (N 35–45° E in Jangada and BR-70, N 50–60° E at Casa de Pedra) is parallel to the regional folded axis and cleavage. (2) Another principle direction (N 130–160° E) is orthogonal to the main regional direction and is almost identical to a later regional fracturing, which produced vertical quartz veins and faults N 130–160° E.

At Jangada, L type aqueous fluid inclusions trails from quartz veins (iii) and host-rocks display somewhat identical rose diagrams, which are dominated by the two systems parallel and orthogonal to the direction of the D4 quartz vein.

At BR-70, several preferential orientations of F.I.T. are superimposed on the above mentioned systems: a N 100° E orientation, dominant in host rocks but absent in folded or D4 quartz veins; a sub-meridian direction (N 0–20° E, N 160–180° E), and a dominant N 140–150° E system of F.I.T. N_2–CH_4 F.I.T. are mostly oriented N 140° E either in folded and D4 quartz veins, whilst aqueous inclusions are oriented preferentially N–S in folded veins and N 130–150° E in D4 quartz veins.

At Casa de Pedra, F.I.T. patterns are less clear but may be interpreted as the result of the superimposition of a N–S (±20°) system on the two orthogonal systems observed everywhere. The N–S system is dominated by aqueous inclusions.

The microcrack patterns result probably from distinct stages of deformation, since most F.I.T. may be interpreted as cracks, with preferential orientations perpendicular to the $\sigma1$–$\sigma3$ plane. A significant part of the F.I.T. display orientations in good agreement with the regional structuring, especially the orientations parallel or perpendicular to cleavage or D4 veins. Other stages of deformation have probably affected the region, especially at BR-70 and Casa de Pedra, and are correlated with the trapping of aqueous fluids in both localities, and N_2–CH_4 fluids in BR-70 in F.I.T. orientated N 150° E to N–S.

F.I.T. displaying similar orientations are present in types (i), (ii), and (iii) quartz veins (N_2–CH_4 F.I.T., for instance). This may indicate that orientations are independent of local anisotropies. However, it is highly probable that complex patterns of F.I.T. may be interpreted partly as the result of local reorientations of stress, and reopening of earlier structures.

Significance of fluid composition

It is worth noting the correlation of early fluid composition with metamorphic grade and host-rock mineralogy. At Casa de Pedra, methane is absent in fluid inclusions. By contrast, BR-70 samples are close to graphite-bearing phyllites
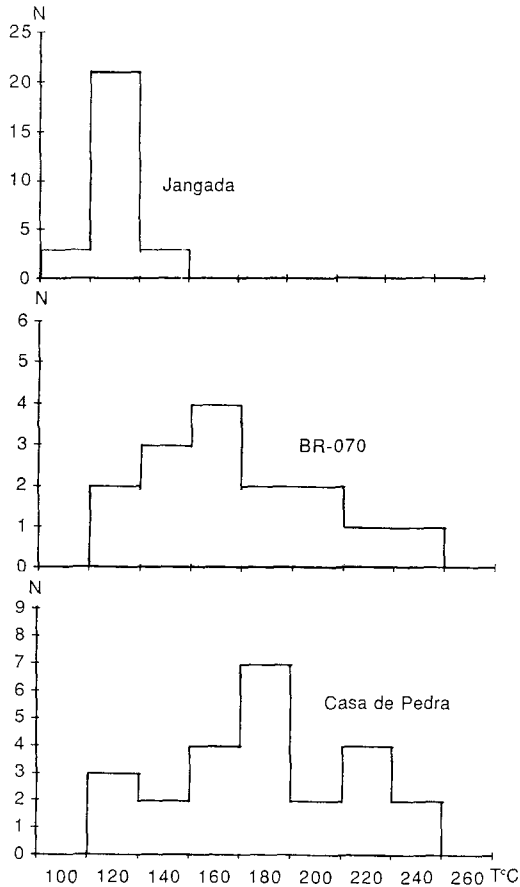
FIG. 4. Distribution of TH data for aqueous inclusions
(L) for the three sample localities.

Table 4. Chemical compositions of H_2O-CO_2 fluid
inclusions from Casa de Pedra. Compositions are given
in mol.%. Tm CO_2 ; melting temperature of CO_2. Th CO_2;
homogenization temperature of CO_2. TH ; homogenization
temperatures. L ; liquid. V ; vapour. d ; density
(g/cm^3). All values for microthermometry in °C.

Type of veins	H2O	CO2	N2	d
(iii)	89	11	0,3	0,75
(iii)	89	10	1	0,75
(i)	91	8	1	0,71
(iii)	68	28	4	0,41
(ii)	85	13	2	0,82

(Fig. 1). Gas analysis shows that the Lc–Vc fluids
at Casa de Pedra, are CH_4 free. This implies
higher f_{O_2} conditions than at BR-70 where CH_4
is always abundant and suggests the early Lc, Vc
and Vn–m fluids carry a fingerprint of peak meta-
morphic conditions in spite of their apparent late
metamorphic origin.

Lcl inclusions with high CO_2 density indicate
fluid pressure between 1 and 2 kbars around
400 °C, calculated from the equations of Kerrick
and Jacobs (1981) and Jacobs and Kerrick (1981).
The spatial association of Lcv and Vc inclusions,
as well as their bulk homogenization tempera-
tures, suggest an immiscibility process around
400 °C and 500 bars (Ramboz *et al.*, 1982). There-
fore, Lcv–Vc inclusions record a decompression
around 400 °C. This temperature is perhaps a little
too high when compared with the degree of meta-
morphism. The presence of the intrusive granite
however, which developed an important meta-
morphic aureole, could be the thermal source
which generated these hotter fluids. Therefore,
the early fluids could be either relic peak meta-
morphic fluids or fluids produced during magma-
tic reheating, or the result of both mechanisms.

The BR-70 locality is characterized by the
absence of high-density fluids (Lcl). The first (Lc)
generation contain a low gas density phase at
room temperature; higher TH values around
340 °C also indicate trapping temperature close
to this value. The second, fluid generation which
are N_2–CH_4 rich and with a very low water content
are probably the vapour phase resulting from an
immiscibility process in the H_2O–CH_4–N_2–H_2S–
CO_2 system at low pressure. The high CH_4/CO_2
ratio can be explained by lower temperatures
which favour CH_4 as the carbon-bearing gas spe-
cies with respect to CO_2 (French, 1966).

At Jangada only aqueous fluids are present.
This may be linked to the lower metamorphic
grade (anchizone–epizone limit), and the litho-
logical nature of the host rocks (quartzites and
carbon-free diamictites). Under such conditions,
production of CO_2, CH_4, and N_2 was not
favoured.

The last episode of fluid circulation is domi-
nated aqueous fluids. At BR-70 and Casa de
Pedra a maximum temperature of 250 °C pre-
vailed, decreasing to a minimum temperature of
130 °C at Jangada. Aqueous fluids at Jangada, are
probably synchronous with the late aqueous fluids
of two previous localities. A similar kind of evolu-
tion is described for Hercynian (France) quartz
veins (Hubert, 1986; Boiron *et al.*, 1988, 1990).

The gold district is restricted to the higher meta-
morphic degree in which CO_2-rich inclusions have
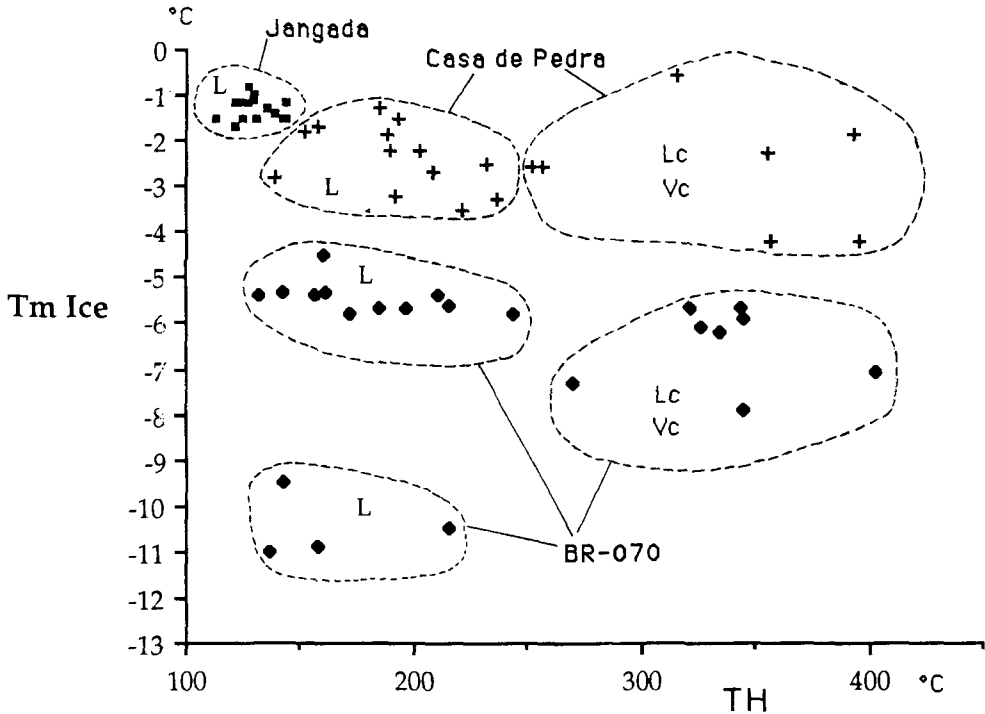been in evidence. However, the understanding

°C

Jangada   Casa de Pedra

Tm Ice

Lc
Vc

L

Lc
Vc

L

BR-070

TH

FIG. 5. Tm H_2O–TH plot for aqueous (L) and H_2O–CO_2 inclusions (Lc).

Table 5 : Directions of the main structures in quartz veins and hosted rocks.

|	Localities	Jangada (C)	BR - 70 (B)		Casa de Pedra (A)	
Host Rock	Type	Quartzite	Phyllite and qztic. intercalations		Phyllites	
	Fold axis (F 1)	40°/8°	40°/10°		60°/10°	
	Cleavage (S 1)	37° 70°	43° 53°		64° 32°	
	Fluid inclusions trails	n=339	n=337			
Quartz Veins	Generation	perpendicular (iii)	Folded (i-ii)	perpendicular (iii)	folded (i-ii)	perpendicular (iii)
	Microcracks		n=135	n=154	n=375	n=205
	Fluid inclusions trails	n=561	n=999	n=1158	n=1140	n=1670
	N2-CH4 trails		n=33	n=35		

(n ; addition of several samples)
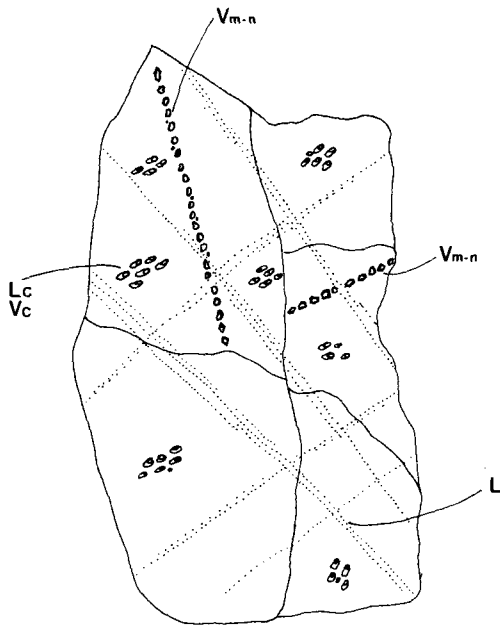
FIG. 6. Relative chronology of fluid inclusions (Lc, Vm-n, L) at BR-70 location, with indication of grain boundaries.

of these fluids in the metallogenic process requires further study.

Conclusions

The main results of this study can be condensed into the following conclusions.

(1) In a given locality, fluid inclusions types are exactly the same in folded quartz veins (i, ii) and non-folded veins (iii). This shows that the earliest fluid generation (Lc–Vc inclusions) to be recorded, is trapped as secondary fluid inclusions during or after the D4 phase. There is no evidence of earlier stages of fluid migration, especially those related to the crystallization of the different quartz veins. This emphasizes the impact of late events on the features of trapped fluids in such environments. Thus, most of the recorded fluid production and migration is linked to thermal or metamorphic events.

(2) The fluid composition of carbonic fluids is correlated with metamorphic grade and host rock mineralogy. Methane is found in carbonic fluid inclusions from samples close to graphite-bearing phyllites at BR-70, whilst Lc–Vc fluids are CH_4 free at Casa de Pedra.

(3) F.I.T. are structural markers of brittle deformation stages, and are probably related to the regional stress fields. F.I.T. orientations parallel or perpendicular to the cleavage are similar to those of mesoscopic fractures, and in agreement with the D4 stress field. However, it is highly probable that preferential orientations other than the above mentioned result from further stages of deformation. The latter are characterized by changes in the orientation of the stress field and are associated with specific fluid migration, especially aqueous fluids and/or N_2–CH_4 at BR-70.

References

Almeida, F. F. M. de and Mantovani, M. S. M. (1975) Geologia e geocronologia do Granito São Vicente, Mato Grosso. *Anais Acad. Brasileira Ciênc.* **47**, 451–8.

Alvarenga, C. J. S. de (1986) Evolução das deformações polifásicas brasilianas na Faixa Paraguai, região de Cuiabá, MT. In *Anais 34th Congr. Brasileiro Geol.*, SBG. Goiânia, **3**, 1170–5.

——(1988) Turbiditos e a glaciação do final do Proterozóico superior no Cinturão Paraguai, Mato Grosso. *Rev. Brasileira Geociênc.* **18**, 323–7.

——and Trompette, R. (submitted) Glacially influenced turbidite sedimentation in the uppermost Proterozoic of the Paraguay belt (Mato Grosso, Brazil). *J. Sedimen. Petrol.*

Boiron, M. C., Cathelineau, M., Dubessy, J. and Bastoul, A. M. (1988) Proceedings of the SIMP meeting, Verbania, Italia, 'Granites and their surroundings', 1987, *Rendiconti Soc. Ital. Min. Petrol.* **43**, 485–98.

——————————(1990) Fluids in Hercynian Auveins from the French Variscan belt. *Mineral. Mag.* **54**, 231–43.

Campos, E. G., Xavier, R. P. and Oliveira, S. M. B. de (1987) Caracterização dos fluidos mineralizantes relacionados aos veios de quartzo auríferos do Grupo Cuiabá. *1° Congresso Brasileiro de Geoquímmica, Porto Alegre, 1987. Anais*, **1**, 417–35.

Crawford, M. L. and Hollister, L. S. (1986) Metamorphic fluids: the evidence from fluid inclusions. In *Fluid–rock interactions during metamorphism* (J. V. Walther and B. J. Wood, eds.) *Advances in Physical Geochemistry*, **5**, 1–35. Springer-Verlag.

Dubessy, J., Poty, B. and Ramboz, C. (1989) Advances in C–O–H–N–S fluid geochemistry based on micro-Raman spectrometric analysis of fluid inclusions. *Eur. J. Mineral.* **1**, 517–34.

French, B. M. (1966) Some geological implications of equilibrium between graphite and a C–H–O gas phase at high temperatures and pressures. *Rev. Geophys.* **4**, 223–53.

Hasui, Y. and Almeida, F. F. M. de (1970) Geocronologia do centro–oeste brasileiro. *Bol. Soc. Brasileira Geol.*, São Paulo, **19**, 1–26.

Hubert, P. (1986) *Texture et inclusions fluids des quartz aurifères. Application au gîte de Cross Gallet (Haute-Vienne, France) et au prospect de Sanoukou (District de Kinieba, Mali).* Thèse Université d'Orleans.

Jacobs, G. K. and Kerrick, D. M. (1981) Methane: an equation of state with application to the ternary system H_2O–CO_2–CH_4 system. *Geochim. Cosmochim. Acta*, **45**, 607–14.

Kerrick, D. M. and Jacobs, G. K. (1981) A remodified Redlich-Kwong equation for H_2O, CO_2 and H_2O–CO_2 mixtures at elevated pressures and temperatures. *Am. J. Sci.* **281**, 735–67.

Kowallis, B. J., Wang, H. F. and Jang, B. (1987) Healed microcrack orientations in granite from Illinois borehole UPH-3 and their relationship to the rock's stress history. *Tectonophys.* **135**, 297–306.

Lapique, M., Champenois, M. and Cheilletz, A. (1988) Un analyseur vidéographique interactif: description et applications. *Bull. Minéral*, **111**, 679–87.

Lespinasse, M. and Pêcher, A. (1986) Microfracturing and regional stress field: a study of the preferred orientations of fluid-inclusion planes in a granite from the Massif Central, France. *J. Struct. Geol.* **8**, 169–80.

Mullis, J. (1979) The system methane–water as a geologic thermometer and barometer from the external part of the Central Alps. *Bull. Minéral.* **102**, 526–36.

——(1987) Fluid-inclusion studies during very low-grade metamorphism. *Low-temperature metamorphism* (M. Frey, ed.), 162–99. Blackie.

Oltra, P. H. (1988) Une nouvelle méthode de quantification de la déformation subie par un échantillon. Apports du traitement numérique d'images et du filtrage de convolution. *C. R. Acad. Sci. Paris*, **306**, 1493–9.

Pêcher, A., Lespinasse, M. and Leroy, J. (1985) Relations between fluid trails and regional stress field: a tool for fluid chronology—an example of an intragranitic uranium ore deposit (northwest Massif Central, France). *Lithos*, **18**, 227–37.

Potter, R. W. (1977) Pressure corrections for fluid inclusion homogenization temperatures based on volumetric properties of the system $NaCl$–H_2O. *J. Res. U.S. Geol. Surv.* **6**, 245–7.

——Clynne, M. A. and Brown, D. L. (1978) Freezing point depression of aqueous sodium chloride solution. *Econ. Geol.* **73**, 284–5.

Poty, B., Leroy, J. and Jachimowicz, L. (1976) Un nouvel appareil pour la mesure des temperatures sous le microscope: l'installation de microthermométrie Chaix-Meca. *Bull. Soc. Fr. Min. Crist.* **99**, 182–6.

Ramboz, C., Pichavant, M. and Weisbrod, A. (1982) Fluid immiscibility in natural processes: use and misuse of fluid inclusion data. *Chem. Geol.* **37**, 29–48.

——Schnapper, D. and Dubessy, J. (1985) The P–V–T–X–f_{O_2} evolution of H_2O–CO_2–CH_4-bearing fluid in a wolframite vein: reconstruction from fluid inclusion studies. *Geochim. Cosmochim. Acta*, **49**, 205–19.

Roedder, E. (1984) *Fluid inclusions. Reviews in Mineralogy*, **12**, 644 pp. Min. Soc. America.

Tuttle, O. F. (1949) Structural petrology of planes of liquid inclusions. *J. Geol.* **57**, 331–56.

Wise, D. U. (1964) Microjointing in basement, Middle Rocky Mountain of Montana and Wyoming. *Bull. Geol. Soc. Am.* **75**, 287–306.

Zhang, Y.-G. and Frantz, J. D. (1987) Determination of the homogenization temperatures and densities of supercritical fluids in the systems $NaCl$–KCl–$CaCl_2$–H_2O using synthetic fluid inclusions. *Chem. Geol.* **64**, 335–50.